Hydrogen abstraction from ethylbenzene by imide-*N*-oxyl radicals with and without O_2: a DFT theoretical study

Roger Arnaud,[a] Anne Milet,[a] Carlo Adamo,[b] Cathy Einhorn[a] and Jacques Einhorn*[a]

[a] *Laboratoire d'Etudes Dynamiques et Structurales de la Sélectivité (LEDSS), UMR CNRS 5616, Université Joseph Fourier, 301 Avenue de la Chimie, BP 53X, F-38041 Grenoble Cedex 09, France*
[b] *Laboratoire d'Electrochimie et de Chimie Analytique, UMR 7575, E.N.S.C.P. 11 rue Pierre et Marie Curie, F-75231 Paris Cedex 05, France*

Received (in Cambridge, UK) 6th June 2002, Accepted 18th September 2002
First published as an Advance Article on the web 25th October 2002

In this paper, we report a theoretical study of the hydrogen abstraction reactions from ethylbenzene by a series of imide-*N*-oxyl radicals. Geometry optimizations and vibrational frequencies were performed using density functional theory at the B3LYP/6-31G(d,p) level. Single-point energy calculations were carried out at the PMP2/6-31G(d,p) and B3LYP/6-311+G(2df,2p) levels. Calculations reproduce experimental trends. In the absence of dioxygen, calculated barriers are not too high to prevent H-abstraction but the process is endothermic. The factors governing the reactivity of nitroxide radicals have been discussed in the scope of the state correlation diagram approach. Moreover, the influence of dioxygen on the mechanism of these reactions has also been studied. Thus, the addition of dioxygen occurs after the H-abstraction by nitroxide radicals and no clear evidence for an energetic barrier to O_2 addition was found. However, in the presence of dioxygen the whole process is exothermic and thus H-abstraction becomes irreversible.

The use of molecular oxygen (dioxygen) for the selective oxidation of organic substrates, especially of hydrocarbons, under mild conditions remains a major challenge for organic chemistry. Dioxygen, in its triplet ground state, has a very low kinetic reactivity toward most organic compounds. Therefore, its use as an oxidant requires catalysts associated, for most of the time, with relatively harsh reaction conditions (*i.e.*, high oxygen pressures and rather severe temperatures). Only few aerobic catalytic oxidations of hydrocarbons under normal pressure and temperature have been described so far, although being highly desirable for technical, economical and environmental reasons.[1] Among them, promising catalytic systems make use of *N*-hydroxyphthalimide **1** associated or not with transition metal complexes.[2] They involve nitroxide type phthalimide-*N*-oxyl free radicals **2**, fairly stable but highly reactive species, evidenced by their EPR spectrum.[2b] Radical **2** has been generated *in situ* from **1** following different procedures, for example: by direct reaction of **1** with dioxygen at 80 °C;[2b] *via* H abstraction from **1** by transition metals–oxygen intermediates,[2d] or *via* room temperature H abstraction from **1** by acetylperoxyl radicals, formed by autoxidation of acetaldehyde.[2e]

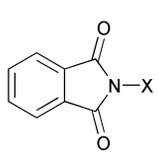

1 X = OH

2 X = O•

The key step in oxidations mediated by **2** is generally supposed to be hydrogen abstraction from the substrate by **2**, generating carbon centered free radicals. These will in turn be readily trapped by dioxygen to provide peroxyl radicals, which will evolve further to the oxidation products. Nevertheless, the key hydrogen abstraction step has, so far, remained a "black box": neither has it been evidenced experimentally nor supported by theoretical investigations. A better understanding of these events would be of importance for the improvement of such catalytic systems. Moreover, we have previously shown that chiral analogs of **1** are promising asymmetric catalysts.[3] For a rational design of more selective catalysts, it would be helpful to know how the corresponding chiral radicals are capable of chiral discrimination. Therefore, the determination of the transition states geometry for such hydrogen abstraction reactions would be a very useful information in future investigations.

Here we report on a theoretical study of hydrogen atom abstraction by imide-*N*-oxyl free radicals, in or without the presence of dioxygen. In order to compare the results with experimental data, we have focused our approach on a benzylic type hydrocarbon such as ethylbenzene, which has experimentally a high reactivity. Concerning the radical species, our aim was to compare phthalimide-*N*-oxyl **2** to other imide-*N*-oxyl radicals such as **3** and **4**: experimentally, indeed, *N*-hydroxyphthalimide **1** exhibits much better catalytic properties than *N*-hydroxyimides associated with radicals **3** and **4**.[2a]

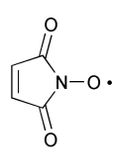

3

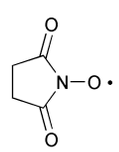

4

For comparison, the study has also been carried out with two other nitroxide-type radicals: on one side dimethyl nitroxide **5**, which is of low stability but is a reasonable computational model for nitroxides having a very low reactivity toward hydrogen abstraction such as di-*tert*-butylnitroxide or 2,2,6,6-tetramethylpiperidine-1-oxyl (TEMPO);[4] on the other side the highly reactive bis-trifluoromethyl nitroxide **6**, able to react even with ethane.[5]

DOI: 10.1039/b205485j

This journal is © The Royal Society of Chemistry 2002

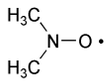

5

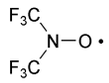

6

As mentioned previously, to the best of our knowledge, there is no evidence of theoretical study of the hydrogen abstraction reaction by imide-*N*-oxyl radicals. However, as hydrogen abstraction is one of the most fundamental reactions of radicals, it has been extensively investigated mechanistically. Radicals involved in theoretical studies other than hydrogen and halogens, are mainly alkyl and silyl radicals,[6] $XO^{\bullet}$ (X = H, F, Cl, Br)[7] and phenyl radicals.[8] Comparison between correlated *ab initio* methods and DFT-based methods indicates that hybrid HF/DFT (B3LYP) provides, for $CH_{4-n}X_n$–YH_3 systems (X = F, C; Y = C, Si), activation energies in good agreement with the experiment.[6a,6b] For the $CH_{4-n}F_n$+$^{\bullet}OH$ hydrogen abstraction reaction, it has been shown that reaction exothermicity and activation energy calculated at the B3LYP level of theory are underestimated with respect to the high level *ab initio* (G2) ones.[7e] The same trend is observed for the reaction of the phenyl radical with methane: the B3LYP reaction energy is less negative (≈3 kcal mol^{-1}) and the B3LYP barrier lower (≈1 kcal mol^{-1}) than the corresponding G2 values.[8a] More recently, Louis *et al.*[7i] in their study of $^{\bullet}OX$–CH_4 (X = Cl, Br) systems established a good agreement between B3LYP and QCISD(T) energy barriers when large basis sets were used. However, in all cases the trends given by B3LYP calculations are in good accordance with those deduced by higher correlated methods. Because of the size of the systems studied here and on the grounds of the above-mentioned results, the use of the B3LYP functional appears to be a good compromise between the reliability of the calculations and the computational effort.

Calculations

All calculations are based on the unrestricted Kohn–Sham (UKS) approach to the DFT[9] as implemented in the Gaussian 98 package[10] using the so-called B3LYP hybrid functional.[11] The structural feature effect of polarization functions on hydrogens has been examined using 6-31G(d), 6-31G(d) augmented by p polarization function only on the abstracted hydrogen and afterwards referred to 6-31G(d*) and 6-31G(d,p) split valence basis set.[12] All of the transition structures have been confirmed by frequency calculations and the corresponding two minima have been established by tracing the intrinsic reaction coordinates (IRCs). Zero-points energies (ZPE) were scaled by 0.9806 (ref. 13) to correct for overestimation of vibrational frequencies.

Basis set effects on relative energies have been tested by UB3-LYP/6-311+G(2d,2p) single-point calculations. Additional post-HF calculations have been made with projected second-order Möller–Plesset (PMP2) method. The electronic structures of the transition structures were analyzed by the natural bond orbital (NBO) method,[14] using the program G94NBO.[15] The adiabatic electronic affinity (EA) of starting radicals have been calculated as the energy difference between ZPE-corrected total energies of the optimized anion and the optimized neutral radical (UB3LYP/6-31+G(d,p) calculations).

Results and discussion

$RNO^{\bullet}$ + ethylbenzene (EB) systems.

In this section, we focus on the results corresponding to the hydrogen abstraction reaction of ethylbenzene (EB) by the radicals **2** to **6**. For all systems, IRC calculations indicate that the TS's are connected to pre-reactive complexes; a schematic reaction path is depicted in Fig. 1. In this discussion, pre-

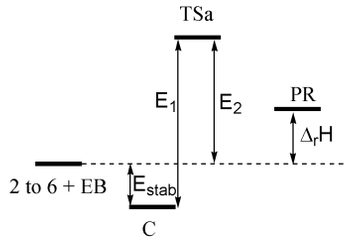

Fig. 1 Reaction profile for hydrogen abstraction by imide-*N*-oxyl radicals from ethylbenzene.

reactive complexes, TS's and products will be referred to as C, TS and PR, respectively.

A representation of the structures of the stationary points is given in Fig. 2 in the case of H-abstraction by radical **3**; similar

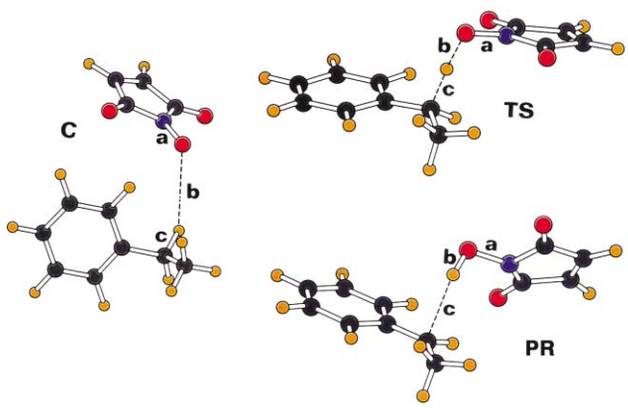

Fig. 2 Optimized structures in the radical **3** + ethylbenzene EB hydrogen abstraction reaction, as obtained at the B3LYP/6-31G(d*) level.

geometries are obtained with the other radicals. The most relevant geometrical parameters are reported in Table 1; the relevant barriers at 0 K defined Fig. 1 are given in Table 2 for the methods employed; the ZPE corrections have been included in all the energy differences.

In all cases, we have found that hydrogen abstractions proceed in one step with TS's characterized by almost collinear arrangement of the three atoms involved in the process (see Fig. 2 and $\angle bc$ values of Table 1 which lies in the range 162–175°). In all TS's, the length of the breaking C–H bond (*c* in Fig. 1 and Table 1) is larger than the forming O–H bond (*b* in Fig. 1 and Table 1). The greatest difference is obtained for the H-abstraction by the radical **5**. To better assess the reactant- or product-like character of the TS, we employ the parameter *L*:[16]

$$L = \frac{c(\mathrm{TS}) - c(\mathrm{C})}{b(\mathrm{TS}) - b(\mathrm{PR})}$$

The lower *L* is, the earlier the transition structure on the reaction coordinate will be; *L* values are also reported in Table 1. The lowest *L* value (*L* = 0.714) is obtained for the H-abstraction by the radical **4** while the highest *L* value (*L* = 2.290) is calculated for the H-abstraction by the radical **5**. The former process is slightly exothermic whereas the latter is the most endothermic (see Table 2). These trends are in accordance with the Hammond's postulate which states that a more exothermic reaction would take place through an earlier transition state.

It is also worth noting that the inclusion of a set of polarization functions on the H abstracted induces a sizeable modification of the geometry of TS, with a lengthening of C–H bond breaking and a shortening of O–H bond forming; as a result, *L*

Table 1 B3LYP optimized values of the most relevant geometrical parameters of the stationary points (pre-complexes C, transition states TS and products PR) for hydrogen abstraction by radicals **2**–**6** from ethylbenzene EB[a b c]

Radicals		Parameters					
		a	b	c	∠ab	∠bc	L
	C	1.265	2.833	1.095	113.4	151.1	
		(1.265)	(2.834)	(1.095)	(113.7)	(151.5)	
2	TS	1.331	1.237	1.318	108.6	173.7	0.875
		(1.334)	(1.227)	(1.338)	(108.2)	(173.6)	(1.008)
	PR	1.372	0.982	2.124	105.3	160.4	
		(1.372)	(0.986)	(2.139)	(105.1)	(161.1)	
	C	1.268	3.027	1.096	129.9	146.6	
3	TS	1.333	1.238	1.317	108.5	174.1	0.853
	PR	1.378	0.979	2.242	105.1	156.0	
	C	1.268	2.695	1.096	97.6	141.8	
4	TS	1.332	1.261	1.296	108.6	173.9	0.714
	PR	1.374	0.981	2.267	105.9	162.1	
	C	1.285	2.632	1.095	120.3	155.1	
5	TS	1.365	1.142	1.466	112.8	164.8	2.290
	PR	1.429	0.980	3.313	107.2	102.9	
	C	1.276	3.949	1.098	58.1	136.9	
6	TS	1.363	1.245	1.327	112.0	175.3	0.887
	PR	1.404	0.987	2.164	107.8	171.8	
	C[d]	1.268	2.815	1.097	93.8	140.8	
3 + $^3O_2$	TSa[e]	1.334	1.237	1.317	108.5	173.8	
	I[f]	1.378	0.980	2.182	105.3	122.1	0.840
	TSb[g]	1.378	0.981	2.175	105.0	151.4	
	PR[h]	1.380	0.975	4.050	105.4	122.1	

[a] Bond lengths are in angstroms and bond angles are in degrees. [b] See Fig. 1 for notation. [c] Values in parentheses calculated with the 6-31G(d) basis set. [d] d = 3.847 Å, e = 1.215 Å. [e] d = 3.589 Å, e = 1.215 Å. [f] d = 3.719 Å, e = 1.214 Å. [g] d = 3.210 Å, e = 1.216 Å. [h] d = 1.491 Å, e = 1.319 Å.

Table 2 Relevant barriers and heat of reaction (including ZPE corrections) for hydrogen abstraction by radicals **2**–**6** from ethylbenzene EB.[a]

Radicals		E_{stab}[b]	E_1[b]	E_2[b]	$\Delta_r H$[b]
	B3LYP/6-31G(d)	−0.8	14.1	13.3	6.3
2	B3LYP/6-31G(d*)	−1.0	11.3	10.3	2.6
	B3LYP/6-311+G(2d,2p)	−0.5	11.5	11.0	3.4
	PMP2/6-31G(d*)	−2.4	10.1	8.1	−3.6
	B3LYP/6-31G(d)	−1.3	13.3	12.0	5.3
3	B3LYP/6-31G(d*)	−2.9	13.1	10.2	2.9
	B3LYP/6-311+G(2d,2p)	−1.4	12.7	11.3	3.7
	PMP2/6-31G(d*)	−5.0	13.6	8.6	−3.1
	B3LYP/6-31G(d)	−4.5	14.0	9.5	2.3
4	B3LYP/6-31G(d*)	−4.6	12.4	7.8	−0.2
	B3LYP/6-311+G(2d,2p)	−2.9	11.7	8.8	−0.6
	PMP2/6-31G(d*)	−6.5	12.4	5.9	−9.6
	B3LYP/6-31G(d)	−5.3	25.9	20.6	17.7
5	B3LYP/6-31G(d*)	−6.9	25.5	18.6	15.1
	B3LYP/6-311+G(2d,2p)	−4.7	25.7	21.0	15.6
	PMP2/6-31G(d*)	−9.6	30.4	20.8	11.4
	B3LYP/6-31G(d)	−2.3	13.8	11.5	4.9
6	B3LYP/6-31G(d*)	−2.6	12.1	9.7	2.4
	B3LYP/6-311+G(2d,2p)	−0.1	11.6	11.5	2.3
	PMP2/6-31G(d*)	−4.1	11.5	7.4	−5.0

[a] In kcal mol^{-1}. [b] For the definition of these quantities, see Fig. 1.

values diminish going from 6-31G(d) to 6-31G(d*) basis set and the product-like character of TS's is reduced (see the case of radical **2** in Table 1). Another point of interest are the relative positions of the two reactants in TSs; in both cases, the phenyl ring of EB and of the imide-*N*-oxyl radicals are *anti* with respect to the C–H–O line. The present point will be helpful for the design of new chiral catalysts. Our first generation of axially chiral radicals possessed a "chiral pocket" on one of their faces. Chiral discrimination occurred when the facially entering substrate interacted with this "chiral pocket".[3] Better selectivities are expected for the next, C_2 symmetric generation of catalysts. The present new information concerning TS's should be very useful for the optimization of the stereoelectronic features of their "chiral pocket".

The B3LYP results in Table 2 indicate that adding one polarization function on the H abstracted to the basis set leads to a decrease both in the reaction enthalpy and in effective activation energy by about 3 and 2 kcal mol^{-1}, respectively. On the other hand, using larger basis set leads to an opposite effect on $\Delta_r H$ and E_2 values, which increase by about 2 kcal.mol^{-1}. With respect to B3LYP/6-31G(d*) energies: (i) E_{stab} calculated at the PMP2/6-31G(d*) level are systematically lower by about 2 kcal mol^{-1}; (ii) PMP2/6-31G(d*) barrier heights are lowered by ≈2 kcal mol^{-1} except for the EB + **5** system for which the opposite trend is established; (iii) PMP2 reaction energies are lowered by 4 to 8 kcal mol^{-1}; this propensity of B3LYP to underestimate reaction exothermicity has been previously observed in both intermolecular[17a] and intramolecular[17b] radical addition to unsaturated substrates. The main topic of this study is the relative reactivities—*i.e.* trends rather than absolute quantities—of radicals **2**–**6** in H-abstraction reactions and all computationals give the same predictions.

On the basis of effective activation energies E_2 at 0 K:[18]

— **5** is obviously the least reactive radical and the H-abstraction by **5** is a very endothermic process;

— **4** is predicted to be the most reactive radical and the H-abstraction reaction is calculated athermic (B3LYP) or weakly exothermic (PMP2);

— the fluorinated radical **6** seems to be little more reactive than the cyclic ones **2** and **3**; the energy profile of the H-abstraction by these two radicals is almost identical and thus **3** appears to be a good model for radical **2**.

These theoretical predictions are in reasonable accordance with experimental observations, except for radicals **3** and **4**. Experimentally, indeed, *N*-hydroxyimides associated with **3** and **4** are poor catalysts.[2a] Nevertheless, an important factor, which has not been taken into account in this study, is the radical stability: radical **2**, although being of the nitroxide type, is not indefinitely stable and its slow decomposition has been studied experimentally.[19] The fact that **2** can be involved in oxidation catalysis implies a favorable balance between its reactivity and stability. This balance seems to be less favorable for **3** and **4**, as these radicals are less stable than **2**.[20]

Now, we will discuss the factors which play a determining role in the reactivity of imide-*N*-oxyl radicals ($X^{\bullet}$) in H-abstraction process:

$$X^{\bullet} + H\text{–}R \longrightarrow X\text{–}H + R^{\bullet}$$

In radical reactions, fundamental factors[21] governing the reactivity are thermodynamic (related to the bond strength of the forming X–H bond if the same substrate is used in all systems), steric and polar (related to the charge polarization in the transition state). Starting from the same substrate, geometrical features of the TS's allow us to assume a minor contribution of steric effect. Using a valence bond (VB) state correlation diagram (SCD) model,[22] Shaik[22c] emphasized the role played by the singlet–triplet excitation energy or the bond energy of the R–H broken bond (related to *G* in Fig. 3) on the

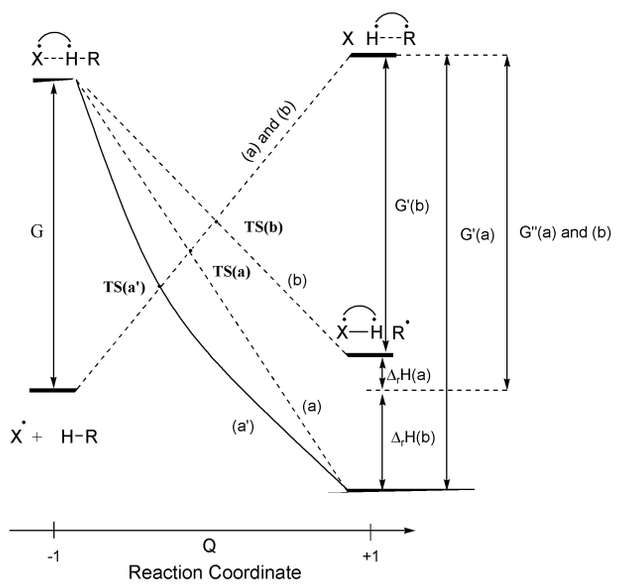

Fig. 3 Correlation diagram for hydrogen abstraction from ethylbenzene by imide-*N*-oxyl radicals (a) exothermic reaction; (b) endothermic reaction.

barrier height. In our systems, this term is constant. In the same way, the *G′* term defined in Fig. 3 can be related to the singlet–triplet excitation energy or the bond energy of the X–H formed bond. The calculated bond energies of the formed bonds BE(O–H) are reported in Table 3.

The heat of the H-abstraction reaction is determined by the strengths of the R–H breaking and X–H forming bonds; insofar as the R–H bond is unchanged one can expect that the variations of *G′* are cancelled by the variations of $\Delta_r H$ and thus the sum $G'' = G' + \Delta_r H$ can be considered as roughly the same in the series. Under this hypothesis, the product diabatic curve is unchanged (see Fig. 3) while the slope of the reactant diabatic curve is $\Delta_r H$ dependent; as a result, $\Delta_r H$ is the organizing quantity of the barriers.

The polar character of the radical, as well as the relative importance of charge transfer configurations X^- $H\text{–}R^+$ or X^+ $H\text{–}R^-$ to the ground-state wave function may be assessed in two ways:

— the computed charge distribution within the TS;

— the ionization energy IP or the electron affinity EA of radical X.

Population analysis (Mulliken and natural population analysis NPA) indicates a charge transfer from H-R to $X^{\bullet}$ in the TS (negative $q(X^{\bullet})$ values in Table 3). All radicals displayed in these processes an electrophilic behavior and the contribution of X^+ $H\text{–}R^-$ configuration can be neglected.

The large negative $q(X^{\bullet})$ values denote a noticeable amount of charge transferred; the weakest charge transfer is calculated for the dimethylnitroxide **5**, the charge transfer associated to other radicals being almost the same. Electron affinities (Table 3) also show a large gap between EA of **5** and those of the other, more electrophilic, radicals. Consequently, it is expected that polar effect is less operative when H is abstracted by **5**, but is otherwise very similar for other radicals.

A plot of barrier height E_2 *versus* enthalpy for the five systems studied is shown in Fig. 4.

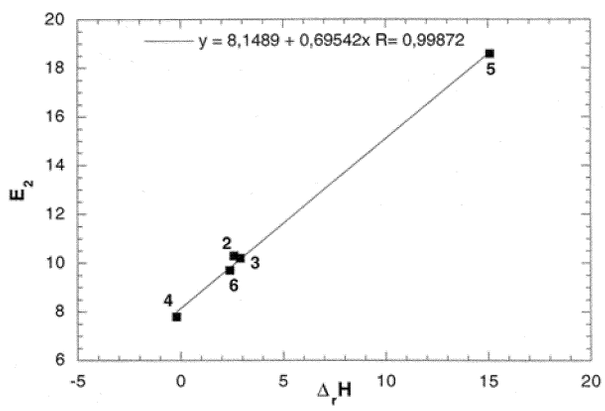

Fig. 4 Plot of barrier height (B3LYP/6-31G(d*) + ZPE, kcal mol^{-1}) against reaction enthalpies for the hydrogen abstraction by radicals **2**–**6** from ethylbenzene.

A very good correlation is obtained ($R = 0.9987$) in accordance with the predictions based on the SCD model. However, the fact that reaction enthalpy correlates with barrier height does not necessarily mean that reactivity is not affected by the polar effect because the polar and enthalpic parameters are not independent but correlate with one another; indeed, a good correlation ($R = 0.9867$) is found between the enthalpy $\Delta_r H$ and the electron affinity (EA). Under these conditions, it is difficult to assess the part of charge transfer stabilization of the transition state on the barrier height.

Finally, we discuss briefly the possible effect of the delocalization of the odd electron of radicals on the relative reactivities. In the scope of the SCD approach, the excited electronic configurations of the reactants have the same spin-pairing patterns as the ground state of the product. When the two spin-paired electrons are gradually coupled in the new O–H bond, the magnitude of the interaction and, hence the slope of the curve joining these configurations, are proportional to the spin density on the atoms to be connected.[23] For a given substrate, it is thus expected that a localized radical gives a larger bond-coupling interaction (and hence a curve which descends steeply toward the crossing point, schematically represented by a dotted line in Fig. 3). The result is that an early TS and a lower energy barrier are obtained in this case. In nitroxide radicals, it is well known that spin delocalization occurs mainly between N and O atoms:

$$R_2N\text{–}O^{\bullet} \leftrightarrow R_2N^{+\bullet}\text{–}O^-$$

Atomic spin density values are given in the last column of Table 3; the dimethylnitroxide **5** possesses the lowest spin

Table 3 Calculated charge-transfer data Δq related to hydrogen abstraction by radicals **2**–**6** from ethylbenzene (EB) and calculated properties of these radicals (electron affinity (EA), O–H bond energy [BE(O–H)] and atomic spin density)

	Δq[a]				Spin density	
Radicals	Mulliken	NPA	EA/eV[b]	BE(O-H)[c]/kcal mol^{-1}	N	O
2	−0.327	−0.366	2.09	77.3	0.200	0.636
3	−0.327	−0.365	1.89	77.8	0.217	0.646
4	−0.329	−0.365	2.11	82.1	0.182	0.647
5	−0.210	−0.257	0.28	68.1	0.419	0.538
6	−0.303	−0.348	2.03	79.7	0.313	0.657

[a] Amount of charge transfer from the radical to EB in the transition structures (UB3LYP/6-61g(d*)). A negative value indicates electron transfer from EB to the radical. [b] Including ZPE. [c] Calculated at the (U)B3LYP/6-311+G(d,p) level at 298.15 K.

density on the oxygen center (0.538), the other radicals having roughly the same spin density on the oxygen atom (≈0.64). The radical delocalization effect leads to a lower reactivity of **5** but does not differentiate the other radicals. Thus, we can conclude that the radical delocalization effect cannot modify the tendency given by the reaction enthalpies.

RNO$^{\bullet}$ + ethylbenzene (EB) + $^3O_2$ systems

In this section we examine the role played by $^3O_2$ on the mechanism of the H-abstraction by RNO$^{\bullet}$ radicals. For this purpose, we have considered radical **3** as a model. Extensive exploration of the potential energy surface indicates that H-abstraction occurs before the addition of $^3O_2$. The energy profile of the whole process is shown in Fig. 5. Some stationary points depicted in Fig. 6 (C, TSa and I) have been located on the quartet PES; expectation values $<S^2>$ of C, TSa and I are 3.750, 3.769 and 3.751, respectively ($<S^2>$ = 3.750 for a pure quartet state).

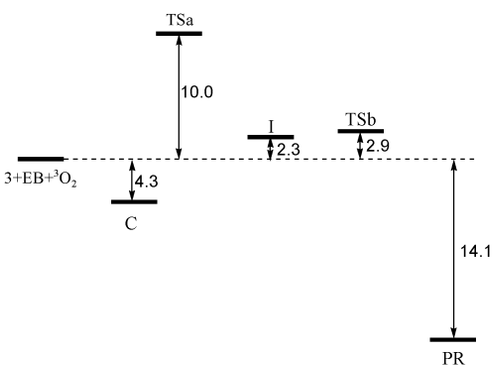

Fig. 5 Reaction profile for hydrogen abstraction by radical **3** from ethylbenzene in the presence of $^3O_2$ (B3LYP/6-31G(d*) + ZPE, kcal mol^{-1})

The main geometrical parameters of these three structures are given in the last entry of Table 1. TSa is reached for a C–O distance *d* equal to 3.589 Å; *b* and *c* distances are the same with and without dioxygen (see Table 1). TSa is connected to the pre-complex C and the intermediate I; during the TSa ⟶I step, O_2 is shifted towards the five-membered ring, the ∠*cd* angle going from 148° (TSa) to 95.7° (I). If one compares the relative position of O_2 in I and PR (Fig. 5), one can deduce that O_2 in I does not possess the suitable orientation to give the peroxyl radical. The relative energies of these stationary points are given at the last entry of Table 2 and the ZPE corrected barriers are indicated in Fig. 5. TSa lies 10.0 kcal mol^{-1} higher than the reactants, a value very close to the one calculated without O_2 (10.20 kcal mol^{-1}). Similarly, the enthalpies $\Delta_r H$ of the H-abstraction step are equal to 2.3 and 2.9 kcal.mol^{-1} with and without O_2, respectively.

Now, we examine the O_2 addition step. We have located on the PES the transition structure TSb (see Fig. 6) obtained for a relatively large distance *d* (3.210 Å *vs* 3.719 Å in I) and for a ∠*cd* angle which increases (109.8° *vs* 95.7° in I). As shown in Fig. 5, TSb lies only 0.6 kcal mol^{-1} higher than I. Beyond this weak barrier, the existence of TSb will be questionable: the expectation value $<S^2>$ computed from the Slater determinant formed from the unrestricted Kohn–Sham orbitals of TSb is equal to 1.763 (0.75 for a pure doublet state). This spin contamination affects the total energy of TSb. We tentatively corrected the UB3LYP energy using the spin-correction procedure proposed by Yamaguchi and co-workers[23] extended to a mixing of doublet and quartet states (assuming that the quartet contamination is the dominant one), although the use of this technique is still a matter of debate.[24] The corrected spin-projected energy E_{SP} is calculated from the following relation:

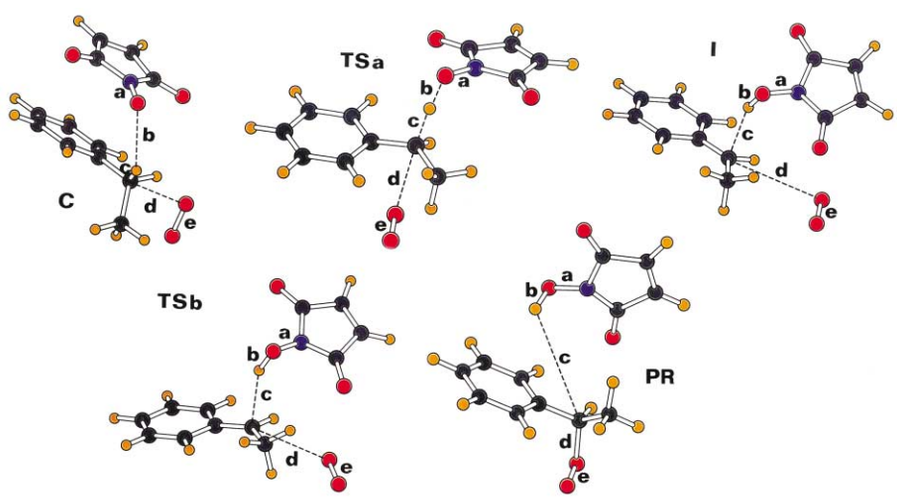

Fig. 6 Optimized structures in the radical **3** + ethylbenzene (EB) hydrogen abstraction reaction in the presence of $^3O_2$ (B3LYP/6-31G(d*) + ZPE, kcal mol^{-1})

$$^2E_{SP} = {}^2E_{UB3LYP} + f_{SC}\left({}^2E_{UB3LYP} - {}^4E_{UB3LYP}\right) \text{ with } f_{SC} \cong \frac{{}^2\langle S^2\rangle_{UB3LYP}}{{}^4\langle S^2\rangle_{UB3LYP} - {}^2\langle S^2\rangle_{UB3LYP}}$$

Taking ESP, the barrier height for the I ⟶Pr step is lowered and becomes equal to 0.2 kcal mol^{-1} only; in addition, extension of basis set still reduces the barrier by 0.1 kcal mol^{-1}. Thus, if the barrier exists, it is very weak and the H-abstraction by **3** is undoubtedly the rate-determining step of the whole process.

The dioxygen addition is achieved in the peroxy radical (PR) which lies 14.1 kcal mol^{-1} below the reactants and thus the whole process becomes exothermic. Therefore, one can conclude that the main role played by $^3O_2$ is to render the H-abstraction reaction irreversible.

Conclusions

In this paper, we have first investigated H-abstraction reactions by various imide-*N*-oxyl radicals using a DFT computational approach based on the B3LYP functional. From a methodological point of view, B3LYP computations reproduce correctly the relative radical reactivities observed experimentally. The calculated barriers are not too high to prevent the H-abstraction, but in the absence of dioxygen the reverse process seems to be favored. Then, we have examined the role played by $^3O_2$ in the H-abstraction process. Our results indicate that $^3O_2$ does not assist the H migration (the activation barrier of the H-abstraction step is nearly the same with and without $^3O_2$). However, in the presence of dioxygen the whole process is exothermic and hence the H-abstraction becomes irreversible. This computational approach also gives an access to geometrical information such as TS geometry, which will be of interest for further investigations concerning chiral radicals.

Acknowledgements

This work was generously supported by the CNRS. A generous allocation of computer time by the CINES is also gratefully acknowledged.

References

1 (*a*) C. L. Hill, *Activation and Functionalization of Alkanes*, Wiley, New York, 1989; (*b*) R. A. Sheldon and J. K. Kochi, *Metal-Catalyzed Oxidations of Organic Compounds*, Academic Press, New York, 1981; (*c*) L. Simandi, *Catalytic Activation of Dioxygen by Metal Complexes*, Kluwer, Boston, 1992; (*d*) D. H. R. Barton, A. E. Martell and D. T. Sawyer, *The Activation of Dioxygen and Homogenous Catalytic Oxidation*, Plenum Press, New York, 1993; (*e*) A. L. Feig and S. J. Lippard, *Chem. Rev.*, 1994, **94**, 759; (*f*) B. A. Arndtsen, R. G. Bergman, T. A. Mobley and T. H. Peterson, *Acc. Chem. Res.*, 1995, **28**, 154; (*g*) F. Gozzo, *J. Mol. Catal*, 2001, **171**, 1.

2 (*a*) Y. Ishii, K. Nakayama, M. Takeno, S. Sakaguchi, T. Iwahama and Y. Nishiyama, *J. Org. Chem.*, 1995, **60**, 3934; (*b*) Y. Ishii, T. Iwahama, S. Sakaguchi, K. Nakayama and Y. Nishiyama, *J. Org. Chem.*, 1996, **61**, 4520; (*c*) Y. Ishii, S. Kato, T. Iwahama and S. Sakaguchi, *Tetrahedron Lett.*, 1996, **37**, 4993; (*d*) Y. Yoshino, Y. Hayashi, T. Iwahama, S. Sakaguchi and Y. Ishii, *J. Org. Chem.*, 1997, **62**, 6810; (*e*) C. Einhorn, J. Einhorn, C. Marcadal and J.-L. Pierre, *Chem. Commun.*, 1997, 447; (*f*) K. Matsunaka, T. Iwahama, S. Sakaguchi and Y. Ishii, *Tetrahedron Lett.*, 1999, **40**, 2165; (*g*) N. Sawatari, T. Yokota, S. Sakaguchi and Y. Ishii, *J. Org. Chem.*, 2001, **66**, 7889; (*h*) For a review, see: Y. Ishii, S. Sakaguchi and T. Iwahama, *Adv. Synth. Catal.*, 2001, **343**, 393.

3 C. Einhorn, J. Einhorn, C. Marcadal-Abbadi and J.-L. Pierre, *J. Org. Chem.*, 1999, **64**, 4542.

4 See: H. G. Aurich, *Nitrones, Nitronates, Nitroxides*, Wiley, New York, 1989, p. 314.

5 (*a*) V. Malatesta and K. U. Ingold, *J. Am. Chem. Soc.*, 1981, **103**, 3094; (*b*) T. Doba and K. U. Ingold, *J. Am. Chem. Soc.*, 1984, **106**, 3958; (*c*) C. J. Rhodes, C. S. Hinds, C. A. Heaton, R. L. Powell, R. E. Banks, B. T. Abdo and S. Rodgers, *J. Fluorine Chem.*, 2002, **113**, 51.

6 See, for examples: (*a*) F. Bernardi and A. Botoni, *J. Phys. Chem. A*, 1997, **101**, 1912; (*b*) A. Bottoni, *J. Phys. Chem. A*, 1998, **102**, 10142; (*c*) J. T. Jodkowski, M.-T. Rayez, J.-C. Rayez, T. Bérces and S. Dóbé, *J. Phys. Chem. A*, 1999, **103**, 3750; (*d*) S. L. Boyd and R. J. Boyd, *J. Phys. Chem. A*, 2001, **105**, 7096.

7 See, *e.g.*: (*a*) K. Miaskiewicz and R. Osman, *J. Am. Chem. Soc.*, 1994, **116**, 232; (*b*) I. Aliagas and S. Gronert, *J. Phys. Chem. A*, 1998, **102**, 2609; (*c*) N. M. Donahue, J. S. Clarke and J. G. Anderson, *J. Phys. Chem. A*, 1998, **102**, 3923; (*d*) M. Schwartz, P. Marshall, R. J. Berry, C. J. Ehlers and G. A. Petersson, *J. Phys. Chem. A*, 1998, **102**, 10074; (*e*) J. Korchowiec, S. Kawahara, K. Matsumura, T. Uchimaru and M. Sugie, *J. Phys. Chem. A*, 1999, **103**, 3548; (*f*) F. Louis, C. A. Gonzalez, R. E. Huie and M. Kurylo, *J. Phys. Chem. A*, 2000, **104**, 8773; (*g*) A. González-Lafont, J. M. Lluch and J. Espinosa-García, *J. Phys. Chem. A*, 2001, **105**, 10553; (*h*) J. R. Alvarez-Idaboy, N. Mora-Diez, R. J. Boyd and A. Vivier-Bunge, *J. Am. Chem. Soc.*, 2001, **123**, 2018; (*i*) F. Louis, T. C. Allison, C. A. Gonzalez and J.-P. Sawerysyn, *J. Phys. Chem. A*, 2001, **105**, 4284.

8 See, for examples: (*a*) I. V. Tokmakov, J. Park, S. Gheyas and M. C. Lin, *J. Phys. Chem. A*, 1999, **103**, 3636; (*b*) J. L. Heidbrink, L. E. Ramírez-Arizmendi, K. K. Thoen, L. Guler and H. I. Kenttämaa, *J. Phys. Chem. A*, 2001, **105**, 7875.

9 R. G. Parr and W. Yang, *Density-Functional Theory of Atoms and Molecules*, Oxford University Press, New York, 1989.

10 M. J. Frisch, G. W. Trucks, H. B. Schlegel, G. E. Scuseria, M. A. Robb, J. R. Cheeseman, V. G. Zakrzewski, J. A. Montgomery, Jr., R. E. Stratmann, J. C. Burant, S. Dapprich, J. M. Millam, A. D. Daniels, K. N. Kudin, M. C. Strain, O. Farkas, J. Tomasi, V. Barone, M. Cossi, R. Cammi, B. Mennucci, C. Pomelli, C. Adamo, S. Clifford, J. Ochterski, G. A. Petersson, P. Y. Ayala, Q. Cui, K. Morokuma, D. K. Malick, A. D. Rabuck, K. Raghavachari, J. B. Foresman, J. Cioslowski, J. V. Ortiz, B. B. Stefanov, G. Liu, A. Liashenko, P. Piskorz, I. Komaromi, R. Gomperts, R. L. Martin, D. J. Fox, T. Keith, M. A. Al-Laham, C. Y. Peng, A. Nanayakkara, C. Gonzalez, M. Challacombe, P. M. W. Gill, B. G. Johnson, W. Chen, M. W. Wong, J. L. Andres, M. Head-Gordon, E. S. Replogle and J. A. Pople, *Gaussian 98*, Revision A6, Gaussian, Inc., Pittsburgh, PA, 1998.

11 (*a*) A. D. Becke, *Phys. Rev. A*, 1988, **38**, 3098; (*b*) C. Lee, W. Wang and R. G. Parr, *Phys. Rev. B*, 1988, **37**, 785; (*c*) A. D. Becke, *J. Chem. Phys.*, 1993, **98**, 5648.

12 Description of basis set and explanation of standard levels of theory can be found in the following: J. B. Foresman and A. E. Frisch, *Exploring Chemistry with Electronic Structure Methods*, 2nd edn. Gaussian, Inc., Pittsburgh, PA, 1996.

13 A. P. Scott and L. Radom, *J. Phys. Chem. A*, 1996, **100**, 16502.

14 A. E. Reed, L. A. Curtiss and F. Weinhold, *Chem. Rev.*, 1988, **88**, 899.

15 E. D. Glendening, A. E. Reed, J. E. Carpenter and F. Weinhold, NBO, Version 3.1, 1988.

16 The parameter *L* has been used in recent theoretical work concerning hydrogen abstraction by radicals (see ref. 6c, 6d, 7b, 7e–i, 8a), and we refer to it for comparison. Bond orders have also been used for the analysis of the reactant- or product-like character of the TS's, with a better behavior at long bond lengths. See: K. N. Houk, S. M. Gustafson and K. A. Black, *J. Am. Chem. Soc.*, 1992, **114**, 8565 and references cited therein.

17 (*a*) R. Arnaud, N. Bugaud, V. Vetere and V. Barone, *J. Am. Chem. Soc.*, 1998, **120**, 5733; (*b*) A. Milet and R. Arnaud, *J. Org. Chem.*, 2001, **66**, 6074.

18 If we assume that the reaction occurs according to a two-step mechanism, fast pre-equilibrium between the reactants and C followed by H-abstraction, the net activation energy of the overall reaction is equal to $E_{TS} - E_{reactants}$; see, for example ref. 7h.

19 C. Ueda, M. Noyama, H. Ohmori and M. Masui, *Chem. Pharm. Bull.*, 1987, **35**, 1372.

20 J. Einhorn, unpublished results.

21 A. B. Shtarev, F. Tian, W. R. Dolbier Jr and B. E. Smart, *J. Am. Chem. Soc.*, 1999, **121**, 7335.

22 For an application of the SCD model to hydrogen abstraction reactions, see: (*a*) A. Pross, H. Yamataka and S. Nagase, *J. Phys. Org. Chem*, 1991, **4**, 135; (*b*) S. Shaik and A. Surki, *Angew. Chem. Int. Ed.*, 1999, **38**, 586; (*c*) S. Shaik, W. Wu, K. Dong, L. Song and P. C. Hyberty, *J. Phys. Chem. A*, 2001, **105**, 8226.

23 (*a*) K. Yamaguchi, F. Jensen, A. Dorigo and K. N. Houk, *Chem. Phys. Lett.*, 1988, **149**, 537; (*b*) S. Yamanaka, T. Kawakami, H. Nagao and K. Yamaguchi, *Chem. Phys. Lett*, 1994, **231**, 25.

24 For an example of thermodynamic and polar effect on hydrogen abstraction, see: A. B. Witbrod and H. B. Schegel, *Chem. Phys. Lett*, 1996, **105**, 6574.